
Soluble poly (methyl methacrylate) composites containing covalently associated zirconium dioxide nanocrystals

Natalia Yevlampieva^{1,*}, Alexander Bugrov^{2,3}, Tatiana Anan'eva³, Mikhail Antipov¹, Evgeny Ryumtsev¹

¹Faculty of Physics, Saint Petersburg State University, Saint Petersburg, Russia

²Faculty of Chemistry, Saint Petersburg State University, Saint Petersburg, Russia

³Institute of Macromolecular Compounds, Russian Academy of Sciences, Saint Petersburg, Russia

Email address:

evlam@paloma.spbu.ru (N. Yevlampieva), bugrov.an@mail.ru (A. Bugrov)

To cite this article:

Natalia Yevlampieva, Alexander Bugrov, Tatiana Anan'eva, Mikhail Antipov, Evgeny Ryumtsev. Soluble Poly (Methyl Methacrylate) Composites Containing Covalently Associated Zirconium Dioxide Nanocrystals. *American Journal of Nano Research and Application*. Vol. 2, No. 5, 2014, pp. 104-111. doi: 10.11648/j.nano.20140205.13

Abstract: Well soluble composite samples of poly(methyl methacrylate) containing hybrid nanoparticles with covalently associated ZrO₂ nanocrystals of an average size of (20±5) nm have been studied by light scattering, viscometry and absorption spectroscopy methods in diluted solutions. Composites were synthesized by two ways: *in situ* bulk polymerization of methyl methacrylate in a presence of ZrO₂, and by polymerization of methyl methacrylate in toluene solution with the dispersed ZrO₂ nanocrystals. Surface of ZrO₂ was preliminary chemically modified by γ -(trimethoxysilyl)propyl methacrylate in both cases. Weight fraction of ZrO₂ in composite samples was varied in the range 1-3 %. Solution properties of composite polymers revealed that a way of monomer polymerization (in bulk or in solution) affect the type of the produced polymer-inorganic hybrids. Sphere like "core-shell" nanoparticles with a single ZrO₂ nanocrystal as a core are mainly formed when polymerization in solution is carried out. Under the conditions of *in situ* bulk polymerization the organic-inorganic particles of significantly larger size with the irregular number of associated ZrO₂ nanocrystals are produced. The size of hybrid nanoparticles in composite samples was determined. Transmission electron microscopy was applied to visualize the difference of ZrO₂ distribution in thin films of the both type composite samples.

Keywords: Organic-Inorganic Composites, Hybrid Nanoparticles, PMMA, ZrO₂

1. Introduction

Development of new nanocomposite polymer materials and improvement of those available are the important trends in modern materials science. Considerable experience accumulated over the last decade in the field of polymer composites with different type inorganic nanoparticles has led to the conclusion that nanoparticles should be bound covalently by polymer to ensure a homogeneous distribution of inorganic component in its matrix [1-3]. Only in this case it is possible to obtain the material with the controlled properties. A great progress in producing of polymer-inorganic oxide (SiO₂, TiO₂, ZrO₂) composite materials have been achieved when the oxides distribution inhomogeneity problems, such as a prevention of their aggregation and build-up of a sufficiently high adhesion at the polymer-inorganic particle interface, were overcome due to of special chemical modification of particles surface prior to their incorporation into polymer. By

means of the required functional groups formation on the surface of inorganic particles a covalent linkage between the polymeric and inorganic components can be obtained. This approach was successfully realized for a range of polymers, and polymer-inorganic oxides composites with novel physico-chemical properties were developed [3-8].

Poly(methyl methacrylate) (PMMA) is the universal polymer that is often used as a matrix material for the nanocomposites creation [1, 2]. In [9, 10] the methods of the synthesis of PMMA-ZrO₂ composites by means of *in situ* bulk polymerization of methyl methacrylate (MMA) in the presence of nanosized ZrO₂ were described, and data on the properties of PMMA-ZrO₂ in films and in thin blocks were reported. A preliminary treatment of ZrO₂ surface with organosilicon compounds before polymerization MMA had been applied for the formation of PMMA-ZrO₂ networks [9, 10]. Modification of PMMA by relatively small amount of covalently bound zirconium dioxide nanoparticles (less 15 wet. %) results in

significant enhancement of its thermomechanical and optical characteristics [3, 9, 10]. The area of potential applications of PMMA-ZrO₂ nanocomposites is extremely wide and extends from dentistry to microelectronics [3].

Practical usage of composite materials with the covalently bound nanoparticles is often faced with the necessity to give a preference only soluble well one. This is dictated by a perspective of multiple utilization of the hybrid polymer-inorganic nanoparticles or by possibility of their reselection. PMMA-ZrO₂ composites have never been considered in this aspect mainly due to they were developed for fabrication of the transparent films with the improved mechanical properties for which a crosslinking of macromolecules by surface-modified inorganic nanoparticles is desirable [9, 10]. However, to find the conditions that lead to formation of PMMA-coated ZrO₂ particles soluble well in organic solvents is also possible. This work is dedicated to one of the possible solutions of this problem.

Herein, we report the results of comparative study of dissolvable PMMA-based composites containing covalently bound ZrO₂ nanocrystals, 20 nm in diameter, synthesized by two ways: *in situ* bulk polymerization of MMA, and by polymerization of MMA in toluene solution with the dispersed ZrO₂ nanocrystals. We'll use the term "nanocrystal" for ZrO₂ as individual compound to distinguish between ZrO₂ and hybrid polymer-inorganic components of PMMA composites, since both are the nanoparticles. γ -(Trimethoxysilyl)propyl methacrylate (TMSPM) was used as the modifier of the surface of ZrO₂.

Our study is mainly aimed at the determination of hydrodynamic properties and structure of the hybrid polymer-inorganic nanoparticles forming in the processes of two different methods of synthesis of PMMA composites. To carry out the above task, we have studied composite samples in diluted solutions by dynamic light scattering, viscometry, and absorption spectroscopy. Transmission electron microscopy (TEM) was utilized for confirmation of the results of study in solution. The unmodified PMMA samples, synthesized at the same conditions as ZrO₂ containing analogues, have been studied also.

2. Experimental

2.1. Objects and Materials

Nanosized crystals ZrO₂ with the narrow distribution were prepared under the hydrothermal conditions [11, 12]. Nanocrystals which shape was close to sphere with the mean

diameter value of (20±5) nm were used. Chemical structure of TMSPM which was applied for modification of ZrO₂ is shown in Fig. 1. The technique of ZrO₂ modification by TMSPM was proposed earlier in [7]. TMSPM reacts with OH-groups on ZrO₂ surface so that silicon-containing part of TMSPM covalently joints to inorganic surface when it another part may be involved to the MMA polymerization process being fully similar to structure of PMMA monomer (Fig.1). From one to three chemical bonds between TMSPM molecule and ZrO₂ surface may be realized according to [10]. 2,2'-Azo-isobutyronitrile (AIBN) was utilized as an initiator of MMA polymerization. TMSPM-coated ZrO₂ nanocrystals have been placed

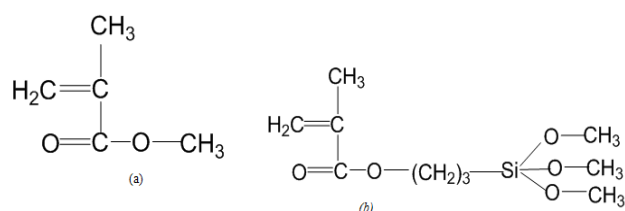


Figure 1. Chemical structure of MMA (a) and TMSPM (b).

to the mixture MMA/ AIBN or mixture MMA/ AIBN/ toluene under the argon atmosphere. Reaction mixture was sonicated (at 3.5 KHz) at room temperature during 20 min, and then the sonication was repeated every hour for 10 min at the corresponding temperature of reaction for a maintenance of high uniformity dispersion of ZrO₂. The content of the compounds in reaction mixtures, temperatures and duration of radical polymerization processes are shown in Table 1. Synthesized composite polymers were precipitated by methanol, and dried under vacuum to the constant weight. Composite PMMA samples containing ZrO₂ presented in Table 1 were completely soluble without any deposition in toluene, benzene, and ethyl acetate.

At the same conditions as the modified samples PMMA-2, 4 (Tabl.1) were received the unmodified samples PMMA-1, 3 have been synthesized in the absence of zirconia component. Composite samples PMMA-5-7 were synthesized in toluene solution under the variable conditions (Tabl.1).

Toluene, ethanol, ethyl acetate (EtAc) ("Vecton", Saint Petersburg, Russia) have been utilized without additional purification. Methanol ("Vecton") was dried and distilled from magnesium methoxide. MMA ("Aldrich") was distilled under normal pressure in argon flow atmosphere. Initiator AIBN was recrystallized from ethanol solution before utilization.

Table 1. Synthesis conditions and yield of polymers.

| Sample | Initial concentration ZrO ₂ (wt.%) | Reaction conditions | Polymer yield (mass %) |
|--------|---|--|------------------------|
| 1 | - | Bulk polymerization *CAIBN=3,8×10 ⁻³ ; 75°C; 45 min | 16 |
| 2 | 1 | Bulk polymerization CAIBN=3,8×10 ⁻³ ; 75°C; 45 min | 14 |
| 3 | - | MMA : toluene=1:1, CAIBN=13×10 ⁻³ ; 75°C; 24 h | 92 |
| 4 | 1 | MMA : toluene=1:1, CAIBN=13×10 ⁻³ ; 75°C; 24 h | 92 |
| 5 | 3 | MMA : toluene=1:1, CAIBN=13×10 ⁻³ ; 75°C; 24 h | 93 |
| 6 | 1 | MMA : toluene=2:3, CAIBN=90×10 ⁻³ ; 60°C; 24 h | 54 |
| 7 | 3 | MMA : toluene=2:3, CAIBN=90×10 ⁻³ ; 60°C; 24 h | 68 |

* C_{AIBN} – concentration of initiator, mol l⁻¹

2.2. Experimental Method

Solution properties of modified and unmodified PMMA samples have been studied in toluene and EtAc at 25 °C. Polymer solutions were prepared at room temperature during 2-3 days.

2.2.1. Optical Properties and Viscosity Determination

UV-V spectra were obtained using spectrophotometer SF-2000 managed automatically by SFScan-program (OKB "Spectr", St.Petersburg, Russia). Quartz cells of 1 cm in length were applied for measurements.

High accuracy microviscometer Lovis-2000 M/ME («Anton Paar», Austria) based on the Heppler method [13] have been used for viscometric measurements. Intrinsic viscosity value $[\eta]$ of polymers was determined in accordance with Huggins procedure *via* a graphical extrapolation of η_{sp}/c value to zero concentration of the solute [14]:

$$\eta_{sp}/c = [\eta] + k' [\eta]^2 c + \quad (1)$$

where η_{sp}/c corresponds to the ratio $(\eta - \eta_0)/\eta_0 c = (t - t_0)/t_0 c$, η and η_0 are the viscosities of a solution and a solvent, respectively; t and t_0 are the time of motion of the ball in a viscometer capillary for solution and solvent, respectively; c is the solute concentration; k' is the Huggins constant corresponding to the slope of the linear dependence $\eta_{sp}/c = f(c)$.

Measurements of solution viscosities have been carried out at the inclination angles of viscometer capillary 45°-65°, where the contribution of gradual dependence to viscosity value was small and comparable with the accuracy of its determination.

Refractometer (Mettler Toledo, Switzerland) with the accuracy ± 0.0001 for refractive index n determination has been applied for measuring of refractive index increments dn/dc . There were received $dn/dc = 0.0109 \pm 0.005$ for PMMA-toluene system and $dn/dc = 0.118 \pm 0.005$ for PMMA-EtAc system. There was not detected any difference in dn/dc values for ZrO₂ containing PMMA samples and for the unmodified PMMA samples in spite of refractive indices of ZrO₂ and PMMA are significantly different. This fact may be considered as a consequence of small enough weight fraction of ZrO₂ in the modified PMMA samples.

2.2.2. Static and Dynamic Light Scattering

The study of static and dynamic light scattering were performed on PhotoCor Complex (PhotoCor, Russia) installations equipped with a real time correlator (288 channels, 20 ns), a goniometer, and a thermostat with a temperature regulation in accuracy within ± 0.05 K. The installations were equipped by the different light sources - lasers with the wavelength 654 nm (power 25mW) and 445 nm (25 mW), correspondingly. The measurements were performed in the range of scattering angles $\theta = 30^\circ - 140^\circ$.

Static light scattering method was used only for measuring of the weight-averaged molecular mass M of the unmodified samples PMMA-1, 3 (Table 1). A basic relationship (2) for the

intensity of the excessive light scattering $I(q, c)$ was applied for data analysis [15]:

$$Hc/ I(q, c) = (1/M) (1 + q^2 R_g^2/3 + \dots) + 2A_2 c + \quad (2)$$

where $q = (4\pi n_0/\lambda_0) \sin(\theta/2)$ is a scattering vector, A_2 is the second virial coefficient, R_g is radius of gyration, $H = 4\pi^2 n_0^2 (dn/dc)^2 / N_A \lambda_0^4$ is an optical constant, n_0 is a refractive index of the solvent, λ_0 is the wavelength of the light source, N_A is Avogadro's number.

Starting from the relationship (2), a Zimm plot (3) have been used for determination of M value [15].

$$Hc/ I(0, c) = 1/M + 2A_2 c \quad (3)$$

Here $I(0, c)$ is a Rayleigh factor determined at $\theta \rightarrow 0$ for all solute concentration c at which the measurements of $I(q, c)$ were performed [15].

M values presented in Table 2 were received from the intercept on y-axis of $Hc/ I(0, c) = f(c)$ according to eq. (3).

The autocorrelation functions of scattered light intensity received in the dynamic light scattering regime were treated with the DynaLS program through the Laplace inverse transform method [16] to obtain the distribution functions of particles in solution over their relaxation times τ .

Translation diffusion coefficients D of the particles in solutions were derived from the slopes of the dependences of the reciprocal relaxation times $1/\tau$ on the squared amplitude of scattering vector q (4) [15].

$$1/\tau = Dq^2 \quad (4)$$

Hydrodynamic radii R of the particles was calculated using experimental D values from the Einstein-Stocks equation (5) [14].

$$R = kT/6\pi\eta_0 D, \quad (5)$$

where k is Boltzmann's constant, T is an absolute temperature.

2.2.3. Transmission Electron Microscopy

TEM samples were prepared by depositing 5 μ L of PMMA solution in EtAc with the solute concentration 0.01 g cm⁻³ onto a Lacey carbon film-coated copper grid. In comparison with a holey carbon films, the Lacey carbon films offer a greater percentage of an open area due to their mesh structure. In drying out process, the polymer sample formed a thin film of approximate thickness of 20 - 40 nm. TEM/STEM imaging was performed on a Zeiss Libra 200 FE transmission electron microscope operated at an acceleration voltage of 200 kV.

3. Results and Discussion

3.1. Solution Properties of Modified /Unmodified PMMA

The vinyl groups of the used organosilicon modifier of ZrO₂ surface are capable of entering into the process of radical copolymerization with MMA (Fig.1), thereby forming a covalent linkage between the inorganic nanocrystals and polymer molecules. During *in situ* bulk polymerization of

MMA, the nanocrystals with an active surface cannot be individually “suspended” to the polymer chains, but may bring about formation of several bonds/cross-links with one or many polymer chains (particle of the “core-shell” type), or build up the network structures that comprise more than one ZrO₂ nanocrystal cross-linked by a number of different macromolecules [9, 10]. Thus, the formation of covalent bonds between PMMA and ZrO₂ through TMSPM may result in both a branched hybrid polymer-inorganic particles and a cross-linked polymer-ZrO₂ networks.

In this study, PMMA samples modified by ZrO₂ were synthesized at different conditions. Not only a polymerization procedure (in bulk or in solution) was varied, but also the ratio solvent/initiator/monomer, as well as a temperature of MMA polymerizing in toluene solution were varied in order to obtain a high yield of the soluble hybrid material (Table 1).

Performing bulk polymerization of MMA in the presence of surface-modified ZrO₂ for more than 55 min resulted in production of an insoluble polymer system. The polymer yield after 45 min from the onset of polymerization, obtained in both the presence and absence of ZrO₂, was not more than 16 wt. % (Table 1). However, a carrying out of MMA polymerization in solution at the same content of ZrO₂ provided a high yield of soluble composite polymer (Table 1).

The molecular properties of the synthesized polymers were studied only for the completely soluble composite samples, which were specially selected. At the beginning of the study the pairs of the unmodified and modified by ZrO₂ PMMA samples, synthesized at the same conditions, have been compared.

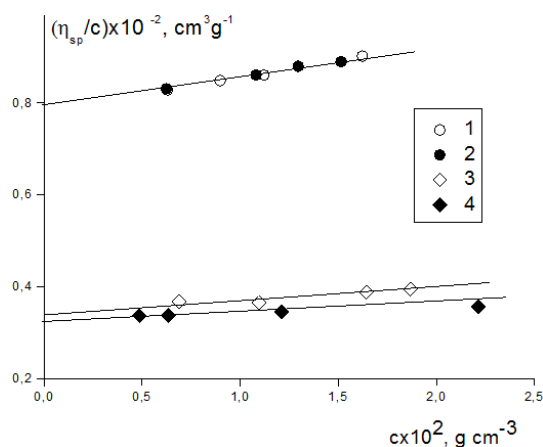


Figure 2. Concentration dependence of reduced viscosity value (η_{sp}/c) for pairs unmodified-modified samples PMMA-1, 2 (1, 2) and PMMA-3, 4 (3, 4) in toluene.

Determination of the intrinsic viscosity value $[\eta]$ in toluene and ethyl acetate (EtAc) revealed that the viscometry is insensitive to presence of ZrO₂ nanoparticles incorporated into the polymer. The concentration dependences of η_{sp}/c value for two pairs of the modified-unmodified PMMA samples in toluene are shown in Figure 2. Both ZrO₂ containing samples PMMA-2 (bulk polymerization) and PMMA-4 (polymerization in solution) are characterized, within the accuracy of measurement, the same $[\eta]$ values as those of the

corresponding unmodified PMMA-1 and PMMA-3. In Table 2 are shown full data of the viscometric measurements for the polymers under investigation.

It is well known that an addition of large-sized foreign particles does not affect the $[\eta]$ value of a polymer if their weight fraction is small or the particles are spherical [14]. Both cases may be the reason of the fact that $[\eta]$ does not change for the studied pairs of PMMA samples. However, first of all, the results of solution viscosity measurements indicate that the main weight fraction in the modified samples corresponds to PMMA molecules of linear structure, and, the second, that weight fraction of the hybrid organic-inorganic particles in the content of these samples is small enough to influence on $[\eta]$ value.

It was ascertained from the studied absorption spectra of the PMMA samples that, in contrast to viscometry, the presence of ZrO₂ in the modified polymers is detected in the spectra and, moreover, the spectra are different for the composite samples synthesized in bulk and in solution.

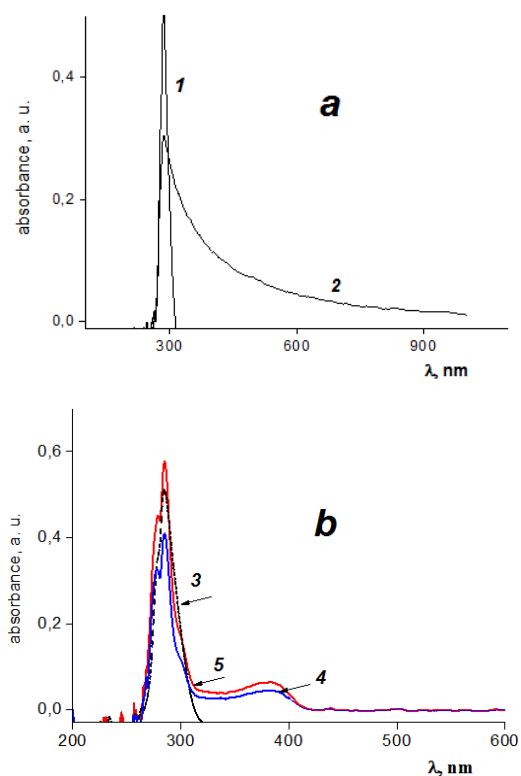


Figure 3. Absorption spectra for PMMA-1 and PMMA-2 at closed values of solute concentration ($\sim 0.4 \times 10^{-2} \text{ g cm}^{-3}$) (a) and corresponding spectra for samples PMMA-3, 4, 5 in toluene solutions (b).

Figure 3a shows the absorption spectra for a pair of PMMA-1 and PMMA-2 prepared by bulk polymerization. The unmodified PMMA-1 absorbs only in the UV spectral range with a characteristic peak at $\lambda=285,5 \text{ nm}$ [17]. Figure 3b shows the absorption spectra of the PMMA-3, 4, 5 synthesized in solution. It can be seen from Figs. 3a and 3b that, for the modified PMMA-4, 5, there is an additional peak in the spectra at $\lambda=383 \text{ nm}$, which is absent in the spectra of the unmodified samples PMMA-1 and PMMA-3. The

appearance of the additional peak in the spectra of the PMMA-4, 5 samples is associated with the absorption by the ZrO₂ surface modified by the organosilicon compound. The presence of the additional peak in the spectra of the modified PMMA asserts the covalent bonding of the ZrO₂ nanocrystals to the polymer chains.

As compared with the spectrum of the unmodified PMMA-1, in that of modified PMMA-2, a change in the spectrum width and the appearance of the arm in the near-*vis* spectral range are revealed (Fig. 3a). The spectrum of the PMMA-2 does not contain a clearly exhibited additional absorption peak, as in the case of the modified PMMA-4, 5 synthesized by polymerization in solution (Fig. 3b). The noted difference in the absorption spectra may be attributed both to the unequal number of inclusions of ZrO₂ nanocrystals in the hybrid polymer-inorganic particles and to a different number of the TMSPM—PMMA bonds in them.

All modified PMMA samples synthesized in solution featured similar absorption spectra. The additional peak at $\lambda=383$ nm was observed in the absorption spectra of PMMA-6, 7 solutions as well, which was of higher intensity than that in the spectra of PMMA-4, 5. This could be an evidence of a difference in the structure of the hybrid particles in these polymers. It should be specially noted that, under the identical synthesis conditions, the intensity of the absorption peak at $\lambda=383$ nm was higher in the case of the PMMA-5 sample (Fig. 3b), which was prepared at a higher content of ZrO₂ than that in the case of PMMA-4 (Table 1). This suggests a potentially possible estimate of the concentration of the hybrid particles in the composition of the modified PMMA samples synthesized in solution from the spectral data.

3.2. A Content of the Modified PMMA Samples

The dynamic light scattering method (DLS) provides determination of the hydrodynamic size and content of various components in solution of heterogeneous polymer [15]. In particular, this can be made for bimodal type distributions in polymer solution. In order to determine weight fractions of the components, the bimodal distributions according to DLS data for spherical particles were theoretically analyzed in [18, 19]. It was also demonstrated that a combination of experimental data from static light scattering (SLS) and DLS could be used for the same task [20, 21].

The algorithm of analysis of the bimodal distributions according to the SLS and DLS data with due account of the peak area ratio was most substantiated and experimentally

validated in [15, 20–22]. It was shown in [20–22] that, when extrapolated to the zero scattering angle q , the S_1/S_2 peak area ratio in the bimodal distribution of the diffusion coefficients D satisfied the following equation

$$(S_1/S_2)_{q \rightarrow 0} = (m_1 M_1)/(m_2 M_2), \quad (6)$$

where m_i and M_i ($i=1, 2$) are the mass quantity of the i -th component in solution and its weight averaged molecular mass, respectively.

According to [23], for Gaussian polymer coils Eq. (6) can be transformed into the form convenient for analysis only from the DLS data.

$$(m_1/m_2) = (S_1/S_2)_{q \rightarrow 0} (R_2/R_1)^{5/3} \text{ good solvent} \quad (7a)$$

$$(m_1/m_2) = (S_1/S_2)_{q \rightarrow 0} (R_2/R_1)^2 \text{ } \theta\text{-solvent} \quad (7b)$$

Here R_i is the hydrodynamic radius of the i -th component.

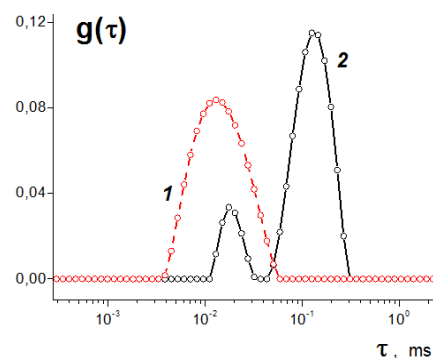


Figure 4. Relaxation time distribution functions for the unmodified sample PMMA-3 (1) and modified PMMA-5 in EtAc at solute concentration $0.46 \times 10^{-2} \text{ g cm}^{-3}$ (2). Scattering angle value is 110° .

Figure 4 shows distribution of the relaxation times obtained from the DLS data for the PMMA-3 and PMMA-5 in EtAc. The distribution is unimodal for the unmodified PMMA-3; hence, the peak of this distribution function is attributed to the ordinary linear PMMA molecules. The relaxation time distribution function in solution of PMMA-5 is bimodal. Besides the particles with the relaxation times corresponding to the PMMA-3 molecules, there are particles of sizes substantially larger than those of PMMA-3 that are present in PMMA-5 solution. The slow and fast (molecular) modes of the distribution presented in Fig. 4 for this polymer correspond to the two types of particles in solution of PMMA-5.

Table 2. Hydrodynamic properties of the studied PMMA samples in toluene and EtAc at 298 K

| Sample | $[\eta] \times 10^{-2}, \text{ cm}^3 \text{ g}^{-1}$ (toluene/EtAc) | $M \times 10^{-3}, \text{ g mol}^{-1}$ | $D \times 10^7, \text{ cm}^2 \text{ s}^{-1}$ | R, nm | w_2^* | n^{**} |
|--------|---|--|--|----------|---------|----------|
| 1 | (0.78/0.62) \pm 0.05 | 350 | 3 (toluene) | 14 | - | - |
| 2 | (0.80/0.58) \pm 0.05 | - | 3 (fast mode)/ 0.3 (slow mode) (toluene) | 14/ 240 | - | - |
| 3 | (0.35/0.26) \pm 0.02 | 120 | 6.2 (EtAc) | 8.3 | - | - |
| 4 | (0.34 /0.27) \pm 0.02 | - | 6.0 (fast mode)/ 0.5 (slow mode) (EtAc) | 8.5/ 100 | 0.02 | 100 |
| 5 | (0.33/0.26) \pm 0.02 | - | 6.2 (fast mode)/ 0.5 (slow mode) (EtAc) | 8.3/ 100 | 0.08 | 108 |
| 6 | (0.17/0.12) \pm 0.02 | 50 | 13 (fast mode)/ 0.5 (slow mode) (EtAc) | 3.8 /100 | 0.05 | 220 |
| 7 | (0.18/0.15) \pm 0.02 | - | 14 (fast mode) /0.6 (slow mode) (EtAc) | 3.5 /83 | 0.07 | 205 |

* w_2 is weight fraction of ZrO₂ containing hybrid macromolecules in the modified PMMA sample;

** n is equivalent number of PMMA molecules attached to the surface of ZrO₂ in PMMA-4-7 synthesized in toluene solution.

The transition from the unimodal to the bimodal particle distribution was typical for all studied unmodified-modified PMMA pairs synthesized in solution and for the PMMA-1-PMMA-2 pair synthesized in bulk. However, for the modified PMMA-2, the distribution peak corresponding to the “slow” particles was very wide as compared with that corresponding to the modified PMMA samples synthesized in solution, i.e, the hybrid particles in the PMMA-2 composition obviously show wider spread in sizes.

Both modes of the relaxation time distributions for the modified PMMA samples are of the diffuse nature, which is seen in Fig. 5 that shows the inverse relaxation time $1/\tau$ as a function of squared sine of half-scattering angle for the PMMA-4 sample. The dependences presented in Fig. 5 are linear and traverse the origin of coordinates. From the slopes of these dependences, the translational diffusion coefficients D were determined according to Eq. (4). The diffusion coefficients D were independent of solute concentration. The concentration-averaged D values and hydrodynamic radii R of the particles calculated by Eq. (5) are presented in Table 2.

As follows from the DLS data (Table 2), the composite PMMA samples contain particles of hydrodynamic sizes corresponding to the size of molecules in the unmodified analogues, and much larger particles of sizes by an order of magnitude and more (in the case of bulk synthesis) exceeding the size of the linear PMMA macromolecules. The large-sized particles should contain ZrO_2 nanocrystals.

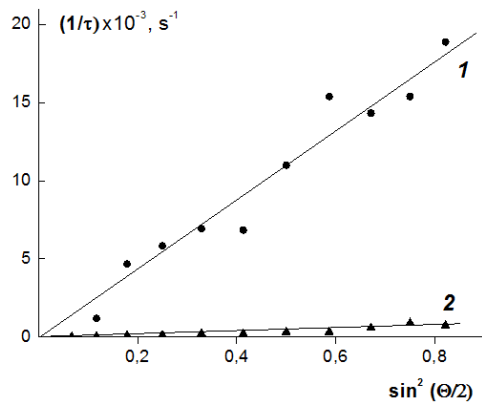


Figure 5. Dependence of the inverse relaxation time values $1/\tau$ versus scattering angle as $\sin^2(\theta/2)$ for the fast mode (1) and slow mode (2) of corresponding distribution function received by DLS for modified sample PMMA-4 in EtAc at solute concentration $0.698 \times 10^{-2} g cm^{-3}$.

It can be readily inferred that, for *in situ* bulk polymerization of MMA, no systemic pattern could be expected in arrangement of polymer molecules covalently bound to ZrO_2 through TMSPM. Therefore, the zirconium-containing particles in the PMMA-2 sample may be in the form of irregular networks with ZrO_2 nanocrystals in its nodes. Obviously, such formations should be of significantly larger size than free PMMA molecules. The irregularity and large number of chemical bonds between PMMA and TMSPM may be responsible for the shape of the absorption spectrum of modified PMMA-2 (Fig. 3a) discussed

above. During synthesis of the modified PMMA in toluene solution, the formation of the hybrid particles of the “core-shell” type with ZrO_2 as the core is more likely.

Conclusion on the structural difference of hybrid particles in PMMA-2 (bulk polymerization) and PMMA-4-7 (polymerized in solution) is based on the results of TEM study. Figure 6 shows the HAADF-STEM images of the specially prepared thin films of zirconium dioxide modified PMMA-2 and PMMA-4 (see, please, experimental part). As easy to observe, the both polymers demonstrate similar images corresponding to homogeneous distribution of ZrO_2 in PMMA matrix in the scale of 1000 nm (Fig.6 (a, c)). More detail images in the scale of 50 nm and 200 nm (Fig. 6 (b, d)) show that zirconia particles in polymer matrix are larger in size and consist of several nanocrystals in PMMA-2 film when a majority of zirconia particles of ~ 20 nm in size are locked separately in the film of PMMA-4.

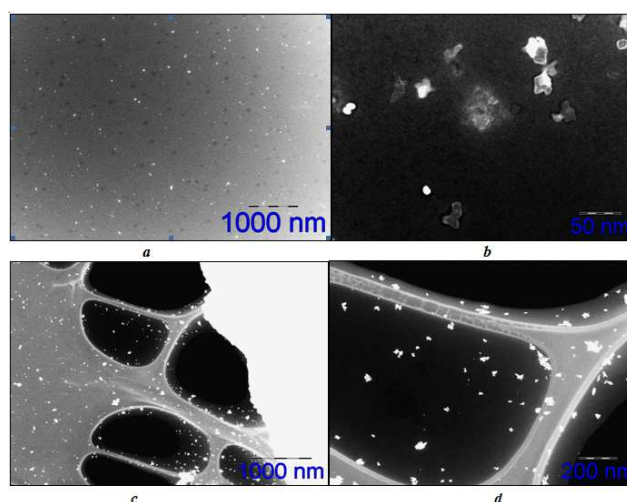


Figure 6. Transmission electron microscope images of thin films of ZrO_2 -containing samples PMMA-4 synthesized in solution (a, b), and PMMA-2 synthesized by *in situ* bulk polymerization (c, d), at the scale variation. Black background corresponds to an open area of the carbon-film-coated copper grid.

The fact that a size of the large particles in PMMA-4-7 synthesized in solution are only by an order of magnitude larger than a free (not connected with ZrO_2) molecule size attests in favor of this statement. Apparently, this may occur due to the growth of a sufficiently large number of the PMMA chains in the direction normal to the ZrO_2 surface. In this case, the macromolecules bound to the nanocrystal will be unable to take the inherent Gaussian coil conformation and will be forced to stretch [24]. Consequently, the size of the hybrid particles essentially differ from those of individual macromolecules in the PMMA-4—7 solutions (Table 2).

For the bimodal distributions of the diffusion coefficients of the particles in the modified PMMA-4—7 solutions, we determined the limits of the peak area ratio (S_1/S_2) at the zero scattering angle $q \rightarrow 0$ (Fig. 7). Using Eq. (7a) for the toluene solutions and Eq. (7b) for EtAc solutions, the (m_1/m_2) ratios were obtained.

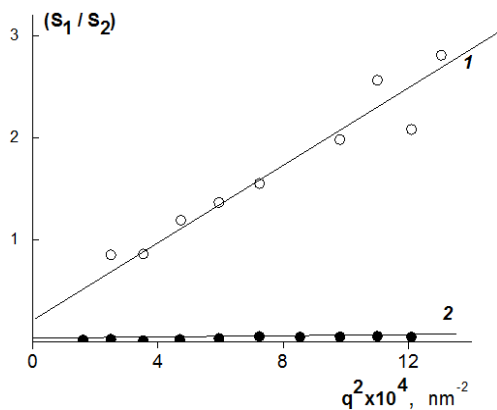


Figure 7. Dependence of peak area ratio (S_1/S_2) of the diffusion coefficient distribution function versus the squared scattering vector q^2 for modified samples PMMA-2 (1) and PMMA-4 (2) in EtAc at solute concentration $0.8 \times 10^{-2} \text{ g cm}^{-3}$.

The total amount of the solute in polymer solution $m=m_1+m_2$ is always known, which, with due account of the additional data on the (m_1/m_2) ratio, makes it possible to determine the weight fraction $w_2=m_2/(m_1+m_2)$ of the polymer-inorganic particles in the composition of the modified PMMA samples. Thereby obtained estimates of the w_2 value are listed in Table 2.

Correlation can be noted between the wt.% content of ZrO_2 nanocrystals in the samples presented in Table 1 and the calculated weight fraction w_2 of the hybrid particles listed in Table 2. As can be seen, the weight fraction of the hybrid particles in the modified PMMA appears fairly small, which properly explains the viscometry insensitivity to their presence in the composite polymers.

Assuming that polymerization degree of the free PMMA molecules and those linked to ZrO_2 through TMSPM should not strongly differ, let us estimate the equivalent number n of the polymer molecules bound to ZrO_2 in the modified samples synthesized in solution.

The M_1 value of the molecular component and (m_1/m_2) ratio being known, Eq. (6) provides the estimation of the mean molecular mass M_2 of the hybrid particles. For the PMMA-6, 7, we estimated the M_1 value using the Mark-Kuhn equation for PMMA in toluene [25] and the experimental value of the intrinsic viscosity of PMMA-6 (Table 2). The M_1 value for PMMA molecules in the content of PMMA-6, 7 was amounted to $50 \times 10^3 \text{ g mol}^{-1}$. By subtracting the mass of the zirconia core and contribution of TMSPM-modifier from M_2 , the mean equivalent number of the PMMA molecules in the hybrid particles of the modified polymers synthesized in solution can be calculated.

The n value was estimated subject to the condition that the ZrO_2 nanocrystals are spherical in form, 20 nm in diameter, and their density is 6 g cm^{-3} [8,11]. The total mass of the bound TMSPM modifier molecules was calculated for the mean density of 10 molecules per nm^2 [9, 10]. The n value was calculated by the equation $n = (M_2 - 25.12 \times 10^{-18} \text{ g} - M_{\text{TMSPM}} \times 12.5 \times 10^3) / M_1$, converting the polymer molecular mass to grams. Thus received n values are listed in the last column in Table 2.

It should be noted that the n value is different for PMMA-4, 5 and PMMA-6,7, that is, for the samples synthesized under varied conditions (see Table 1). This fact is the evidence of the effect of temperature and concentration of initiator in the reaction mixture on the number of PMMA molecules covalently associated with ZrO_2 , since the density of the bound TMSPM molecules per unit surface of nanocrystals was not varied. In this case, it appeared that the size of the hybrid particles in the PMMA-4,5 and PMMA-6, 7 samples are close to one another. The latter confirms the above inference that the polymer chains are forced to acquire the elongated conformations when being attached to ZrO_2 nanocrystals through TMSPM. Hence, the extent of their elongation may increase as the density of the attachments increases.

Note also that the masses of the inorganic and organic parts of the hybrid particles in PMMA-4-7 are practically equal to each other. Therefore, only those modified polymers are completely soluble which contain ZrO_2 nanocrystals with covalently bound polymer whose total mass is close to the mass of the nanocrystals proper. Apparently, this specificity provides high solubility of the hybrid particles in organic solvents, and it is an important factor for creating uniform distribution of inorganic particles in a polymer matrix.

4. Conclusions

In conclusion, it can be stated that the conditions of MMA polymerization in a presence of surface-modified ZrO_2 nanocrystals affect the type of the formed polymer-inorganic particles in a final PMMA composite. During MMA polymerization in toluene solution, mainly the “core-shell” hybrid particles are formed with ZrO_2 as the core. In a process of *in situ* bulk polymerization of MMA, the hybrid particles of the irregular cross-linked structure are formed of considerably larger size than those formed during polymerization in solution. Synthesis of a composite PMMA material in solution may be preferable if compared with that in bulk, because a higher yield of a polymer containing soluble hybrid polymer-inorganic particles can be obtained under these conditions.

Acknowledgements

The authors are grateful to Interdisciplinary resource center for nanotechnologies of St. Petersburg State University where TEM imaging was performed and also grateful to St. Petersburg State University Center for Diagnostics of functional materials for medicine, pharmacology and nanoelectronics for the dynamic light scattering measurements.

References

- [1] D. Vollath, “Nanomaterials: An introduction to Synthesis, Properties and Applications”, 2d ed., New York: Wiley, 2008, 386 pp.

- [2] S. Pavlidou and C.D. Papaspyrides, "A review on polymer-layered silicate nanocomposites", *Progress in Polymer Science*, 2008, vol. 33, pp. 1119-1198.
- [3] K. Friedrich, S. Fakirov and Z. Zhang, "Polymer Nanocomposites: From Nano- to Macro-scale", New York: Springer, 2005, 367 pp.
- [4] V.E. Yudin and V.M. Svetlichnyi, "Effect of the structure and shape of filler nanoparticles on the physical properties of polyimide composites", *Russian J. General Chem.*, 2010, vol. 80, pp. 2157-2169.
- [5] S. M. Khaled, R. Sui, A. Paul, P.A. Charpentier and A.S. Rizkalla, "Synthesis of TiO₂-PMMA Nanocomposite: Using Methacrylic Acid as a Coupling Agent", *Langmuir*, 2007, vol. 23, pp. 3988-3995.
- [6] P. Obreja, D. Cristea, V.S. Teodorescu, A. Dinescu, A.C. Obreja, F. Comanescu and R. Rebigan, "Preparation and patterning of nanoscale hybrid materials for micro-optics", 2010, vol. 12, pp. 2007-2013.
- [7] A.N. Bugrov, E.N. Vlasova, M.V. Mokeev, E.N. Popova, E.M. Ivankova, O.V. Almjashaeva and V.M. Svetlichnyi, "Distribution of zirconia nanoparticles in the matrix of poly(4,4'-oxydiphenylene-pyromellitimide)", *Polym.Sci. Ser. B.*, 2012, vol. 54, pp. 486-495.
- [8] S. Shokoohi, A. Arefazar and R. Khorsokhavar, "Silane Coupling Agents in Polymer-based Reinforced Composites: A Review", *J. Reinf. Plast. Comp.* 2008, vol. 27, pp. 473-485.
- [9] Y. Hu, S. Zhou and L. Wu, "Surface mechanical properties of transparent poly(methyl methacrylate)/zirconia nanocomposites prepared by in situ bulk polymerization", *Polymer*, 2009, vol. 50, pp.3609-3616.
- [10] T. Otsuka and Y. Chujo, "Poly(methyl methacrylate) (PMMA)-based hybrid materials with reactive zirconium oxide nanocrystals", *Polymer J.*, 2010, vol. 42, pp. 58-65.
- [11] A.N. Bugrov, "Polymer-inorganic composites based on carbon and heterochain polymers modified by ZrO₂ nanoparticles", PhD Thesis, St.Petersburg, 2013.
- [12] O.V. Pozhidaeva, E.N. Korytkova and D.P. Romanov, "Formation of ZrO₂ Nanocrystals in Hydrothermal Media of Various Chemical Compositions". *Russian J. General Chem.* 2002, vol. 72, pp. 849-853.
- [13] A. Ya. Malkin and A.E. "Diffusion and viscosity of polymers. Measurements methods" Moscow: Chemistry, 1979, 304 pp.
- [14] V.N. Tsvetkov, "Rigid-chain polymers: Hydrodynamic and Optical properties in solution", New York: Consultants Bureau, 1989, 397 pp.
- [15] B. J. Berne and R. Pecora, "Dynamic Light Scattering", New-York: Courier Dover Publication, 2000, 376 pp.
- [16] <http://photocor.com/dynals/>
- [17] N.V. Agrinskaja, E.G. Guk, I.A. Kudrjajtsev and O.G. Ljublinskaja, "Spectral study of polydiacethylene-THD in PMMA matrix", *Phys. Solid State*, 1995, vol. 37, pp. 969-975.
- [18] S. Okabe, S. Sugihara, S. Aoshima, and M. Shibayama, "Heat-Induced Self-Assembling of Thermosensitive Block Copolymer. Rheology and Dynamic Light Scattering", *Macromolecules*, 2003, vol.36, pp. 4099-4106.
- [19] M. Shibayama, T. Karino and S. Okabe, "Distribution analysis of multi-model dynamic light scattering data", *Polymer*, 2006, vol. 47, pp. 6446-6456.
- [20] C. Wu, M. Siddiq and K. F. Woo, "Laser Light-Scattering Characterization of a polymer Mixture Made of Individual Linear Chain and Clusters", *Macromolecules*, 1995, vol. 28, pp. 4914-4919.
- [21] Y. Zhang, C. Wu, Q. Fang and Y.-X. Zhang, "A Light-Scattering Study of the Aggregation Behavior of Fluorocarbon-Modified Polyacrylamides in Water", *Macromolecules*, 1996, vol. 29, pp. 2494-2497.
- [22] C. Wu, S. Bo, M. Siddiq, G. Yang and T. Chen, "Laser Light-Scattering Study of Novel Thermoplastics. 2. Phenolphthalein Poly(ether sulfone)" *Macromolecules*, 1996, vol. 29, pp. 3157-3160.
- [23] E.A. Litmanovich and E.M. Ivleva, "The problem of bimodal distributions in dynamic light scattering: Theory and experiment", *Polym. Sci. Ser. A.*, 2010, vol. 52, pp. 671-678.
- [24] A.A. Mercurieva, T.M. Birshtein and V. M. Amoskov, "Theory of Liquid-crystalline ordering in polymer brushes", *Macromol. Symp.*, 2007, vol. 252, pp. 90-100.
- [25] S.N. Chinai, J.D. Matlack, A.L. Resnick and R.J. Samuels, "Poly(methyl methacrylate): Dilute solution properties by viscosity and light scattering", *J. Polym. Sci.*, 1955, vol.17, pp. 391-401.